Tetrahedron 68 (2012) 8276–8285

Contents lists available at SciVerse ScienceDirect

Tetrahedron

journal homepage: www.elsevier.com/locate/tet

Unprecedented double benzylic rearrangement: regio- and stereospecific tandem 1,4-shift and Curtin rearrangement

Ángel M. Montaña [a,*], Stefano Ponzano [a,†], Consuelo Batalla [a], Mercè Font-Bardia [b,c]

[a] Industrial and Applied Organic Chemistry Research Unit, Department of Organic Chemistry, University of Barcelona, c/Martí i Franquès 1-11, 08028 Barcelona, Spain
[b] Department of Crystallography, Mineralogy and Mineral Deposits, University of Barcelona, c/Martí i Franquès s/n, 08028 Barcelona, Spain
[c] Unitat de Difracció RX, Centre Cientific i Tecnològic (CCiTUB), Universitat de Barcelona, c/Solé Sabarís 1-3, 08028 Barcelona, Spain

ARTICLE INFO

Article history:
Received 11 June 2012
Received in revised form 13 July 2012
Accepted 16 July 2012
Available online 24 July 2012

Keywords:
Benzyl ethers
Benzylic rearrangement
Enolates
1,2-Shift
1,4-Shift
Curtin rearrangement
Wittig rearrangement

ABSTRACT

An α-benzyloxyketone forming part of a strained cyclopentane carbon framework when treated with 10 equiv of anhydrous NaOH in absolute ethanol, for 2 h, affords in a 65% yield a new 2-benzyl-2-hydroxyketone, resulting from an unprecedented double benzylic rearrangement. This new rearrangement could be interpreted as an initial benzylic 1,4-shift between the *O*-enolate alkoxide of the ketone group and the oxygen atom of the benzyloxy ether, followed by a Curtin type benzylic 1,2-shift. Apart from the novelty and the synthetic application of this transformation it is worth noting the complete regio- and stereoselectivity observed. The structures of both substrate and product have been confirmed by X-ray diffraction studies. A tentative mechanism is herein proposed.

1. Introduction

Benzylic rearrangements are important in organic chemistry and have been described in a wide variety of chemical transformations and mechanisms. Thus, benzyl ethers undergo [1,2] and [2,3] Wittig rearrangements[1,2] when treated with butyl lithium (Fig. 1). α-Alkoxy-stannanes and α-alkoxy-silanes undergo [1,2] Wittig–Still rearrangements[3] under similar conditions (Fig. 2). Also benzyl shifts are observed in benzyl ammonium salts in the presence of sodium amalgam (Stevens rearrangement)[4] (Fig. 3). On the other hand, β-benzyl silanes in α,β-unsaturated ketones undergo a 1,2-migration of benzyl group from silicon to carbon atom upon treatment with TBFA in anhydrous polar solvents.[5] This silicon-based 1,2-benzylic shift is highly stereoselective (Fig. 4). Finally it is worth noting the Curtin rearrangement[6] (Fig. 5) that takes place in α-benzyloxyketones to afford α-benzyl substituted α-hydroxyketones, by heating the substrates with 1 M potassium hydroxide in ethanol. These strong reaction conditions induced further reactions of the initially-formed products to generate several fragmentation products. For this reason this rearrangement, discovered by Curtin more than 60 years ago, did not have synthetic applications until recently when L.A. Paquette et al.[7] found an interesting rearrangement of an α-benzyloxyketone when synthesizing C10-alkylated toxoids, to afford an unexpected product with high yield (94%) and regio- and stereoselectivity (Fig. 6).

We came across with a similar reaction when synthesizing the precursor **2** of antitumor oxabicyclo[6.2.1]undecanes **4** via an aldol cyclization of methylketones **1**, under strong basic conditions.[8] However, in our case we observed an unexpected and unprecedented double benzylic rearrangement: a 1,4-shift followed by a 1,2-benzylic shift in a regio- and stereoselective manner.

2. Results and discussion

In the synthesis of oxatricyclo[6.2.1.0^{2,6}]undecan-4-one derivatives **2**, by an intramolecular aldol cyclization process (Fig. 7), cyclization of methyl ketone **1** was carried out at room temperature by using 10 equiv of NaOH in absolute ethanol for 8–24 h. The conversion fell within the range of 80–100% and the yield was normally high, 80–95%, depending on the size and bulkiness of group R.

In the particular case of R=benzyloxy, (**1d**), the yield of cyclic aldol **2d** was 95% in 15 h at room temperature. The remaining 5%

* Corresponding author. E-mail addresses: angel.montana@ub.edu (Á.M. Montaña), sponzano@hotmail.com (S. Ponzano), mercef@sct.ub.es (M. Font-Bardia).
† Present address: Department of Drug Discovery and Development, Istituto Italiano di Tecnologia, Via Morego 30, 16163 Genova, Italy.

0040-4020/$ – see front matter © 2012 Elsevier Ltd. All rights reserved.
http://dx.doi.org/10.1016/j.tet.2012.07.053

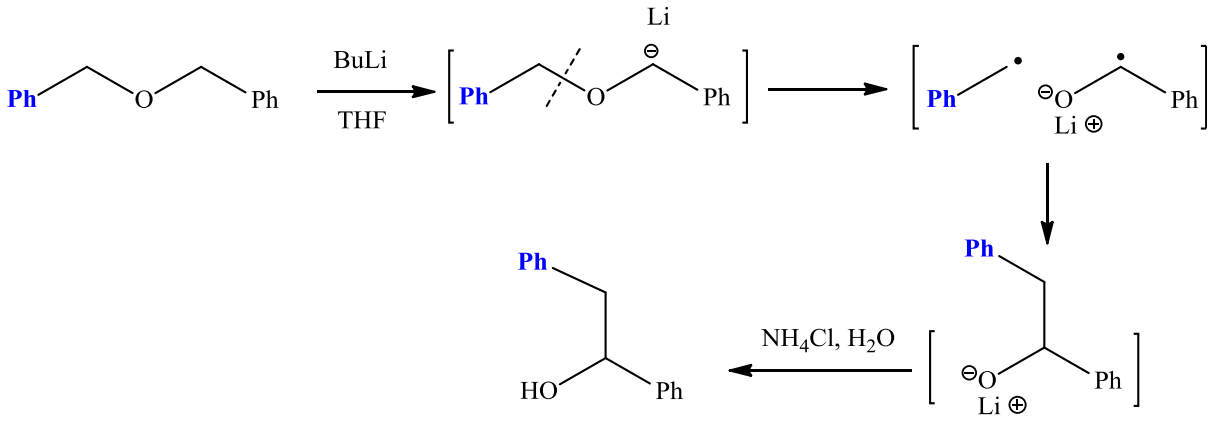

Fig. 1. [1,2] Wittig rearrangement.

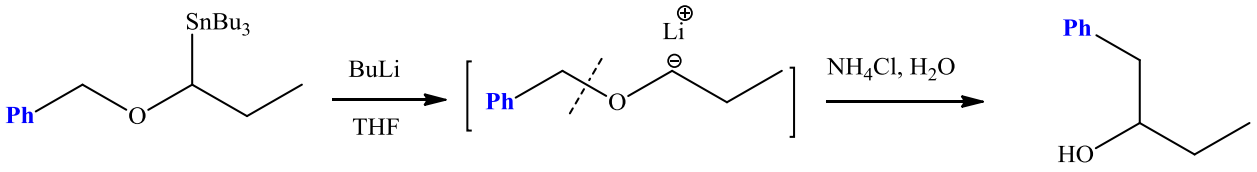

Fig. 2. [1,2] Wittig–Still rearrangement.

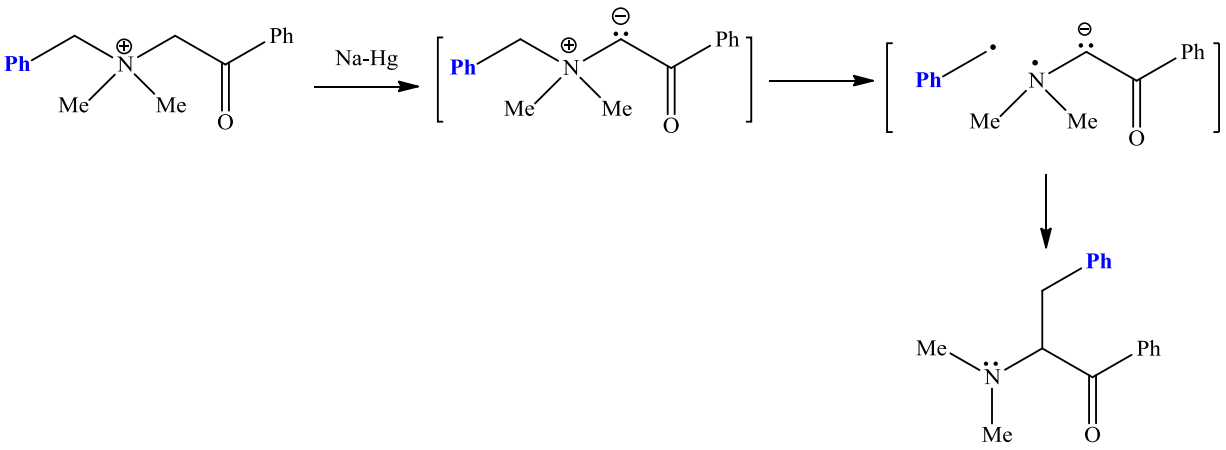

Fig. 3. Ammonium-based 1,2-benzylic shift: Stevens rearrangement.

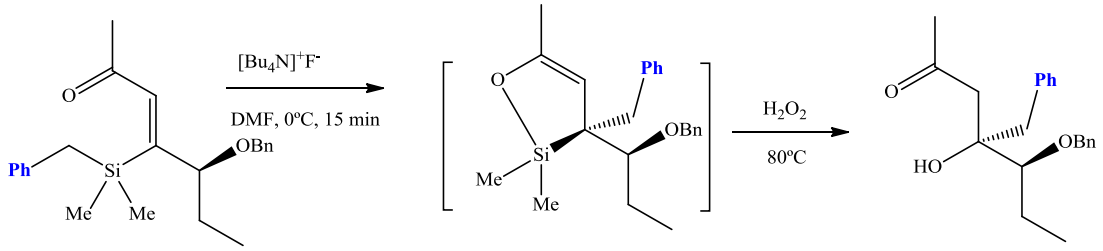

Fig. 4. Silicon-based 1,2-benzylic shift.

was unchanged starting material **1d** that was recovered and reused. The usual work-up procedure comported careful neutralization of the crude reaction mixture with HCl 1 M, removal of EtOH, addition of water, and extraction with ether.

As some times it happens in science our finding was a consequence of serendipity, when we accidentally heated, while concentrating the reaction crude to dryness, and before neutralizing the reaction mixture. In that occasion the work-up protocol was thus inverted and consequently a high concentration of NaOH in EtOH was reached while heating. We observed the formation of a new product **3** in 44% yield, together with our usual aldol product **2** in 30% yield (Fig. 8).

We tried to emulate the new reaction conditions that afforded the new product **3** and also tried to optimize the yield by using the

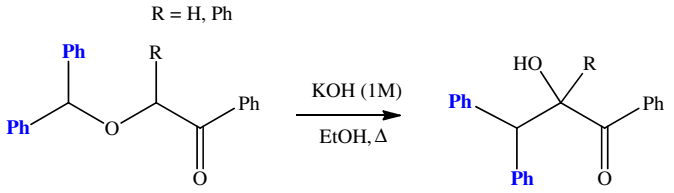

Fig. 5. Curtin rearrangement.

takes place only for high concentrations of base (entries 1–3), no matter of the reaction time. These findings moved us to think that the parameters evaluated do not condition the reaction outcome, due to **3** is generated from **2**, not from **1**, and because the formation of **3** takes place during work-up and not during aldol cyclization. This was confirmed by performing the reaction several times and at different scales, using the right standard protocol, which afforded compound **2** as the only product and with isolated yields (by column chromatography) of 86–95%.

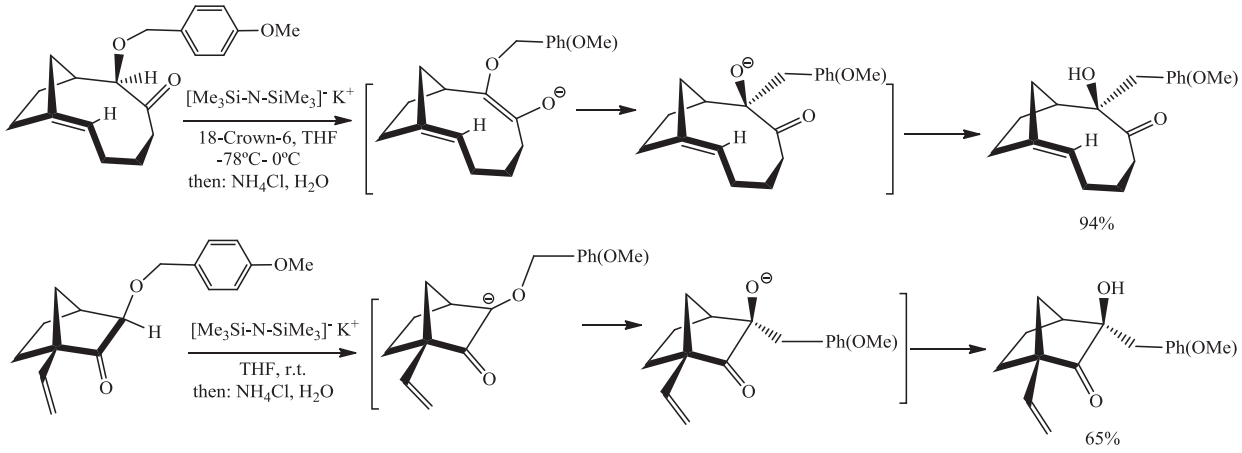

Fig. 6. Synthetic applications of Curtin rearrangement: examples from Paquette's work.

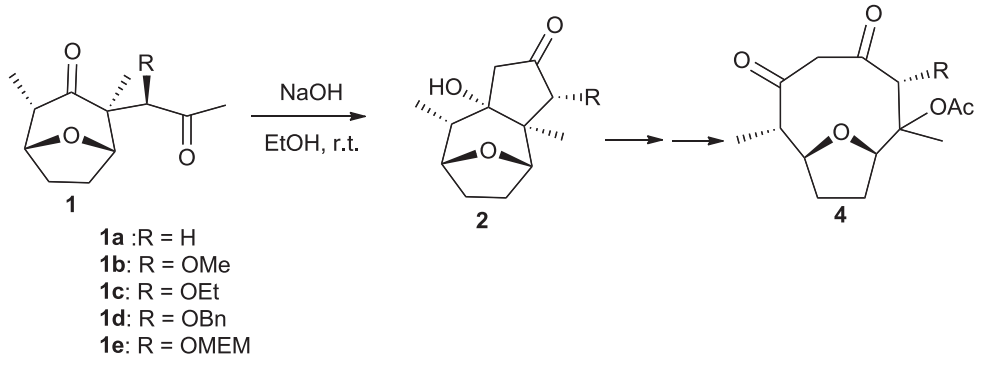

Fig. 7. Synthesis of oxabicyclo[6.2.1]undecanes **4** from precursors **1** and **2**.

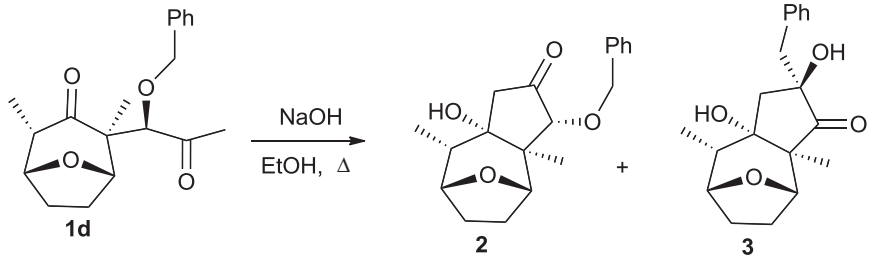

Fig. 8. Unexpected formation of **3** from **2**, during work-up of the aldol cyclization of **1d**.

'inverted protocol'. We evaluated different parameters like: scale of **1** (from 40 to 300 mg), concentration, reaction time (from 10 min to 15 h), molar ratio substrate/NaOH (from 1:1 to 1:10), nature of used base (NaOH or Li–HMDS), and reaction temperature (−78 °C to 40 °C). The results are quoted in Table 1 for comparative purposes.

Observing the results from Table 1 it is possible to conclude that the scale of reaction is not relevant and that the formation of **3** takes place only for high concentrations of base (entries 1–3), no matter of the reaction time. These findings moved us to think that the parameters evaluated do not condition the reaction outcome, due to **3** is generated from **2**, not from **1**, and because the formation of **3** takes place during work-up and not during aldol cyclization. This was confirmed by performing the reaction several times and at different scales, using the right standard protocol, which afforded compound **2** as the only product and with isolated yields (by column chromatography) of 86–95%.

To convert directly **2** into **3**, we reacted pure compound **2** with NaOH in absolute ethanol (**3**/NaOH=1:10) at 2 M concentration, obtaining compound **3** in a 65% yield (Fig. 9). The remaining mass was unchanged product **2**.

Both compounds were separated by flash column chromatography and physically and spectroscopically characterized, and the ^{1}H and ^{13}C NMR data assigned and correlated by COSY and HSQC

Table 1
Trials of the intramolecular aldol reaction of **1** under the new reaction conditions

Entry	Scale of **1** (mg)	Scale of **1** (mmol)	Solvent (mL)	Time	NaOH (equiv)	Li-HMDS (equiv)	Concn of base (mol/L)	*T* (°C)	**2** (%)	**3** (%)	**1** (%)	Conv. (%)
1	100	0.316	EtOH (12)	15 h	10	—	0.260	rt	46	14	40	60
2	300	0.948	EtOH (40)	2.3 h	10	—	0.240	rt	30	44	26	74
3	40	0.126	EtOH (5)	45 min	10	—	0.250	rt	43	35	22	78
4	40	0.126	EtOH (5)	45 min	1.05	—	0.026	rt	27	0	73	27
5	40	0.126	EtOH (20)	22 h	1.05	—	0.006	rt	39	0	61	39
6	40	0.126	EtOH (20)	10 h	1.05	—	0.006	rt	37	0	63	37
7	40	0.126	EtOH (5)	90 min	1.05	—	0.026	rt	23	0	77	23
8	40	0.126	EtOH (5)	45 min	0.5	—	0.013	rt	9	0	91	9
9	40	0.126	THF (3)	10 min	—	1.05	0.044	rt	0	0	100	0
10	40	0.126	THF (3)	24 h	—	1.1	0.046	rt	0	0	100	0
11	40	0.126	THF (3)	72 h	—	2	0.080	−78 to rt	0	0	100	0

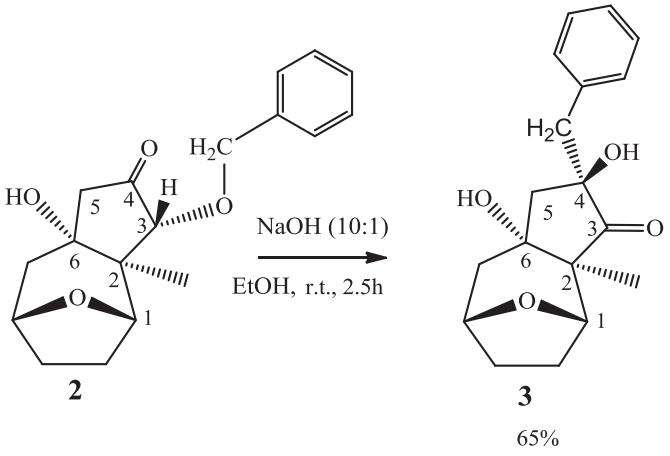

Fig. 9. Direct obtention of **3** by rearrangement of **2** in the presence of NaOH (10:1) in absolute EtOH.

spectra. In the NMR spectra of **3**, it was not observed any signal corresponding to a hydrogen geminal to the benzyloxy group (like H3 in **2**), which usually appears at a chemical shift between 4 and 5 ppm. Another peculiarity of this, then unknown, product **3** was the position in the ^{1}H NMR spectra of the benzylic CH_2 hydrogen atoms. The typical two doublets appeared around 3 ppm, while this kind of hydrogens usually appear in ^{1}H NMR of **2** in the zone of 4–5 ppm.

Thus, the information obtained from NMR studies confirmed that product **3** bore a benzyl group at a different position with respect to the substrate **2**. From the HSQC experiment, a C–H carbon was missing, which inferred its possible transformation into a new quaternary carbon atom. This was confirmed by the totally decoupled ^{13}C NMR spectra. Two new singlets appeared in the ^{1}H NMR spectrum registered in deuterated benzene, without any C–H correlation in the HSQC two-dimensional spectra. These two singlets showed no C–H correlation due to the absence of protons on the carbons that carry the hydroxyl groups (C4 and C6 in **3**).

To unveil the structure of **3** and to compare it with that of **2**, single crystals of both compounds were obtained and analyzed by X-ray diffraction analysis, that showed us a surprising and unexpected structure for **3**, which then could be envisioned as the result of an unusual rearrangement process (Figs. 10 and 11).

It is worth noting that analogues of methylketones **1** (with R=H, OMe, OEt, MOM) have been reacted under these conditions and no rearrangement products analogue of **3** have never been observed. Thus, it is immediate to conclude that this type of rearrangement, under strong basic conditions, is related to the presence of the benzyloxy group. Is for this reason that we looked for similar transformations in the literature and we found only two references regarding this process: one from 60 years ago by D.Y. Curtin[6] and other from 13 years ago by L.A. Paquette,[7] both of them related with a 1,2-benzylic shift, as mentioned in the Introduction section, but none of them could explain the whole observed transformation of **2** into **3**. Other striking result was the complete regio- and stereoselectivity observed: a possible regioisomer **3′** (Fig. 12) has not been detected at all and, on the other hand, the configuration at C4 of **3** is *S**. No epimer in this position has been detected, after a meticulous and careful screening of reaction crudes by NMR, GC, and GC–MS techniques.

A possible mechanism, which could justify the formation of product **3** is represented in Fig. 12. Once the cyclic aldol **2** is formed, the base abstracts the most acidic hydrogen, situated in the α-position to the carbonyl group (C-4) and geminal to the benzyloxy group on C-3, to generate the corresponding delocalized enolate anion **A**. It is envisioned an initial abstraction of H-3, α to the ketone group on C-4, by NaOH due to its pK_a in EtOH medium is 18.46 (calculated by the SPARC computer program)[9] instead of an alternative abstraction of a benzylic hydrogen H-1′ because of its much higher pK_a=32.77 (see Table 2).[9,10] This great difference of acidity (by a factor of 10^{14}) prompted us to propose the mechanism illustrated in Fig. 12.

At this point, to justify the migration of the benzylic group, two consecutives benzylic shift reactions should take place: (a) one 1,4-benzyl shift[11] originated from the oxyanion of enolate **A** on the spatially nearby and partially positively charged carbon (C-1′) of the benzylic group, to generate a second enolate anion **B**; the second one coming from the carbanion of the newly formed enolate **B** on the benzylic carbon (C-1′) via a transitory oxirane ring **C** with the resulting cleavage of the carbon–oxygen bond and the formation of a new carbon–carbon bond (intermediate **D**). The new oxyanion generated would then abstract a proton from water during the work-up process to generate **3**.

One important aspect that remains to be unveiled in our process and also in the reaction described by Paquette et al.[7] is the explanation of the regio- and stereospecificity observed in the formation of the rearranged product.

The 1,4-benzylic shift could be envisioned as a stepwise or as a sigmatropic rearrangement. The approach of 1–4 termini could be rationalized on the basis of the electron density (Hückel charge of benzylic carbon is +0.1317e and that of *O*-enolate oxygen is −0.5790e) and the distance through space between both atoms ($Ph–CH_2\cdots O^-$=2.812 Å). The second step would be the 1,2-benzylic shift (Curtin rearrangement) that would afford (through transition state **C**) intermediate alkoxide **D**, which after aqueous work-up will yield product **3** in a stereoselective manner. In our case and also in Paquette's work, in a first look, it is not clear how starting from a planar enolate **B** (due to resonance stabilization between *C*- and *O*-enolate) it is possible to generate a chiral quaternary center on C4 in a stereoselective way. One may appeal to the different energy of the transition states (type **C**) leading to both theoretically possible epimers at the new stereogenic center

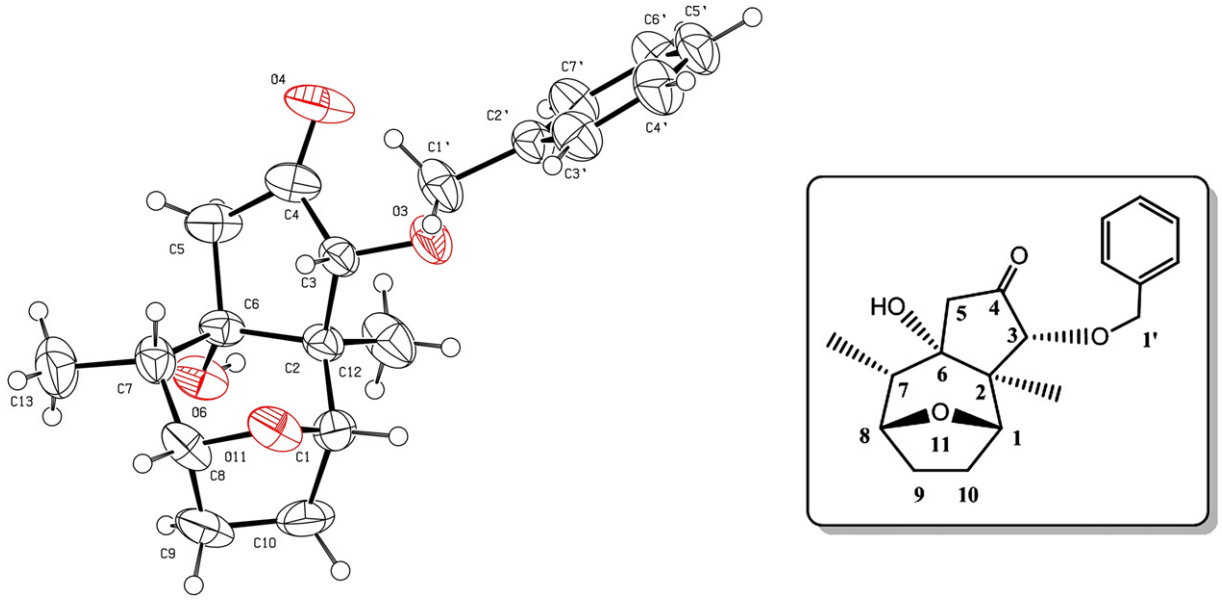

Fig. 10. ORTEP representation of the oxatricyclic precursor **2**.

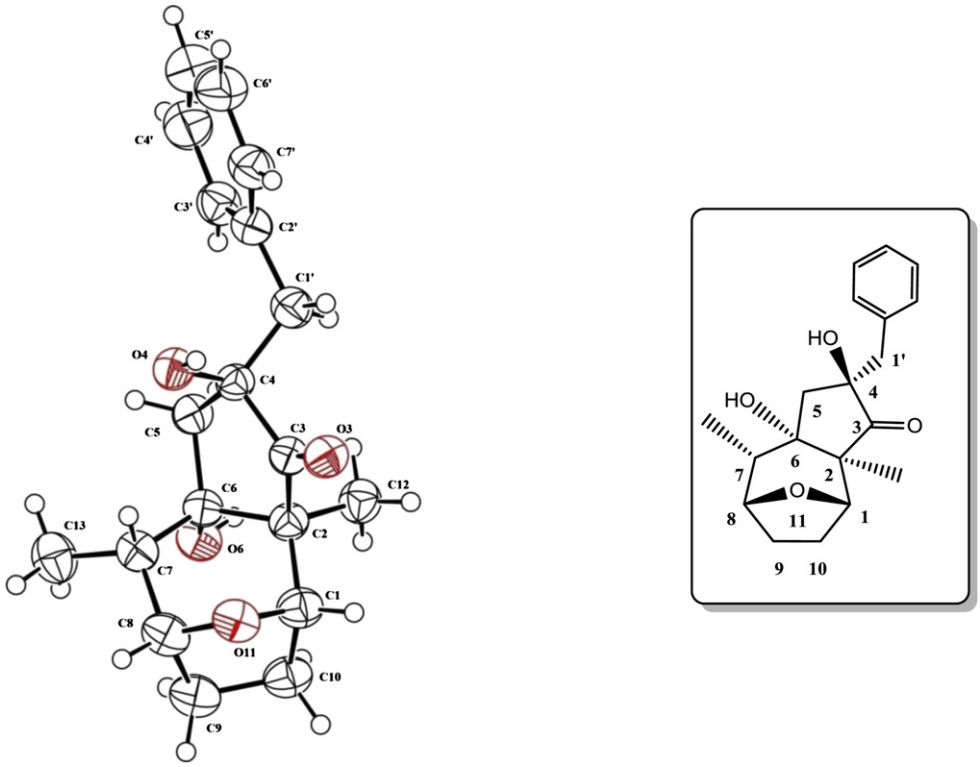

Fig. 11. X-ray structure of the rearrangement product **3**.

(C4), resulting from the attack of the HOMO orbital of the enolate **B** to the LUMO σ* orbital of the C–O bond at the benzylic carbon (Fig. 13). In Table 3, it is possible to observe how the most energy-favorable transition state is TS-2, with lower activation energy and higher ΔH_f (in absolute value), which affords the formation of compound **3**. [12]Also the energy of the four TS has been calculated by the DFT (B3LYP, 6-311^{++}G) method.[13] TS-3 and TS-4 leading to the non-formed isomer **3**″ are less energetically favored. On the other hand, in both types of TS it is worth to mention that TS-2 is preferred to TS-1 and thus is TS-3 over TS-4. This could be due to the *exo* disposition of the phenyl group with respect to the bridging oxygen of the TS, which minimizes steric constraints and propitiates the right orientation of orbitals and the HOMO–LUMO interaction (Fig. 13).[14]

An alternative mechanism to explain the formation of **3** from **2** could be a two-step process consisting in a Curtin rearrangement to generate **3**′, in first place, followed by an α-ketol rearrangement[15] to afford **3**. The stereochemistry of the first Curtin process could be determined on the basis of the energy of the TS, as mentioned before, which also conditions the stereochemical outcome of the acyloin rearrangement due to the right disposition of the benzylic methylene, oriented toward the *Si* face of the carbonyl group.

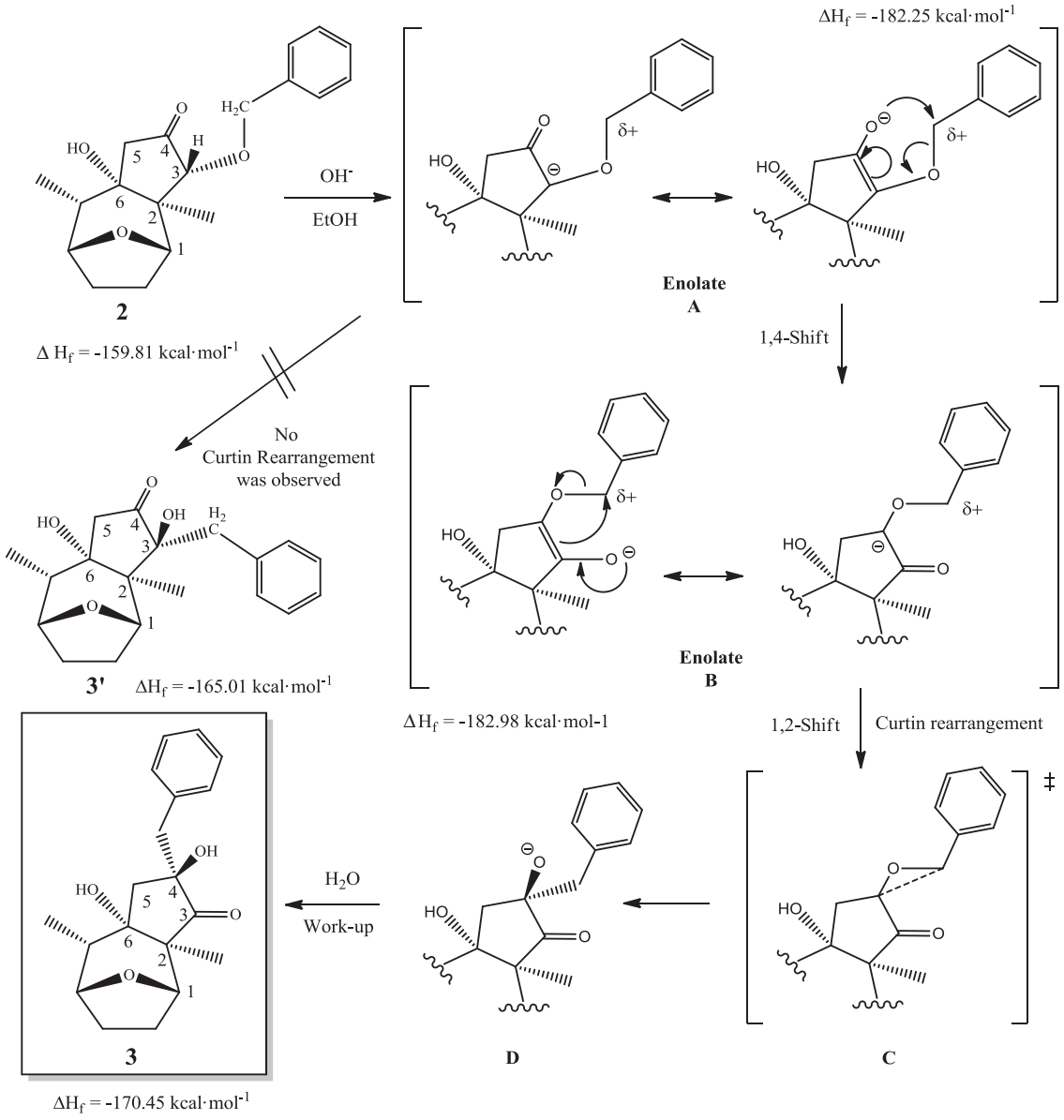

Fig. 12. Mechanism proposal for the formation of product **3**.

Table 2
pK_a values of acidic hydrogens in 3

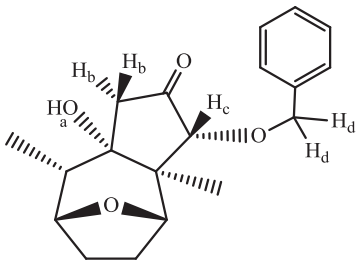

Hydrogen	pK_a (in water)[9,10]	pK_a (in EtOH)[9]	pK_a (in THF)[9]
H_a	17.14	24.14	36.54
H_b	19.96	20.71	31.46
H_c	*15.78*	*18.46*	*29.21*
H_d	34.10	32.77	43.12

However, we have discarded this alternative mechanism as we have never detected the formation of **3′**. Moreover, the driving force of the α-ketol rearrangement usually is the release of the strain of cyclic systems (or very sterically crowded structures) having the α-hydroxyketone functionality[13] but in our case the cyclopentanone substructure remains intact. One question remains without answer: why none of the substrates illustrated in Fig. 6 that underwent a Curtin rearrangement afforded a further 1,4-sigmatropic shift[11] or an α-ketol rearrangement?

On the other hand, a mechanism based on a radical pair dissociation–recombination as proposed for [1,2]-Wittig rearrangements,[1c–e] in our opinion could not be applied in the present case, because the nature of substrates and the reaction conditions make more feasible a heterolytic bond breaking with generation of ionic intermediates. For this reason a stereospecificity involving retention at the migrating center and inversion of the free radical-alkoxide-bearing terminus, proposed for the [1,2]-Wittig rearrangement, cannot be appealed.[16] Finally, it could be addressed the possibility that the reaction proceeds via a heterolytic cleavage pathway similar to that of the anionic oxy-Claisen's rearrangement.[17]

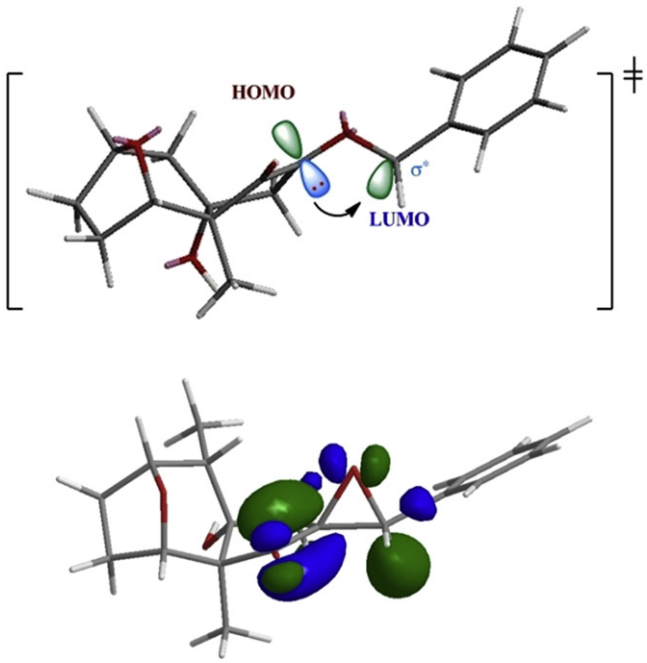

Fig. 13. HOMO–LUMO approach in the TS of the Curtin rearrangement.

3. Conclusions

An unexpected and unprecedented double rearrangement of an α-benzyloxyketone has been observed when reacted with 10 equiv of anhydrous NaOH in absolute ethanol, for 2 h, affording in a 65% yield a new 2-benzyl-2-hydroxyketone. This new rearrangement could be interpreted as an initial benzylic 1,4-shift between the *O*-enolate alkoxide of the ketone group and the oxygen atom of the benzyloxy ether, followed by a Curtin type benzylic 1,2-shift. Apart from the novelty and the synthetic application of this transformation it is worth noting the complete regio- and stereoselectivity observed. The structures of both substrate and product have been confirmed by X-ray diffraction studies. A tentative mechanism is herein proposed.

We consider that the results presented here have sound experimental support for the usefulness of Curtin type base promoted α-benzyloxyketone rearrangements in organic synthesis. Even though reactivity patterns should be screened and theoretical studies should be accomplished in order to understand the complete regio- and stereoselectivity, sufficient understanding and empirical data are available to encourage synthetic chemists to use the Curtin rearrangements, in general, and the herein described methodology in their synthetic planning. Further efforts to expand the scope of this rearrangement to other substrates, and to unveil the reaction mechanism are under way in our laboratory.

4. Experimental section

4.1. General methods

Unless otherwise noted, all reactions were conducted under an atmosphere of dry nitrogen or argon in oven-dried glassware. All solvents were purified using standard techniques before use: ether, tetrahydrofuran, hexane, and pentane were distilled under nitrogen from sodium/benzophenone. Acetonitrile was distilled under nitrogen from CaH_2. Infrared spectra were recorded on an FT-IR NICOLET 510 spectrophotometer as thin films over NaCl. NMR spectra were taken in $CDCl_3$ on VARIAN spectrometers at 200 MHz (GEMINI-200), 400 MHz (MERCURY-400), and/or 500 MHz (UNITY-500) for ^{1}H NMR, and at 50 MHz and 100 MHz for ^{13}C NMR. For ^{1}H NMR tetramethylsilane was used as internal standard. ^{13}C NMR spectra were referenced to the 77.0 ppm resonance of chloroform. Mass spectra were measured on a HEWLETT-PACKARD 5890 mass spectrometer using chemical ionization. GC analyses were performed on HP-8790 gas chromatograph equipped with a HEWLETT-PACKARD-crosslinked 5% MePhe-Silicone capillary column (L=25 m, D=0.2 mm, thickness=2.5 μm) using helium as a carrier gas and an FID detector (T=250 °C, P_{H_2} = 4.2 psi, P_{air}=2.1 psi). The elemental analyses were obtained in a FISONS elemental analyzer, Model Na-1500. The samples were previously pyrolized at 1000 °C under oxygen atmosphere and the content of carbon and hydrogen was determined by evaluation of the combustion gases by gas chromatography using an FID detector.

4.2. X-ray diffraction analyses

Suitable crystals (0.2×0.1×0.1 mm) from compounds **2** and **3** were selected and mounted on a CAD4-Enraf-Nonius and a MAR345 apparatus, respectively, with image plate detector. Unit cell parameters were determined from automatic centering of reflections and refined by least-squares method. Intensities were collected with graphite monochromatized Mo Kα radiation. Lorentz-polarization and absorption corrections were made.

The structure was solved by direct methods and refined by full-matrix least-squares method using SHELXS-97 computer program,[18] on the basis of the non-equivalent reflections by symmetry (very negative intensities were not assumed). The function minimized was: $\Sigma w[(F_o)^2-(F_c)^2]^2$, where $w=[\sigma^2(I)+(0.0591P)^2]^{-1}$ for **2** and $w=[\sigma^2(I)+(0.0555P)^2+0.1371P)^{-1}$ for **3**. $P=[(F_o)^2+2(F_c)^2]/3$; f, f' and f'' were taken from the International Tables of X-ray Crystallography.[19] All the H atoms were computed and refined, using a riding model, with isotropic temperature factor equal to 1.2 times the equivalent temperature factor of the atom, which are linked. The final R (on F) factors and goodness-of-fit are shown in Table 4. The number of refined parameters was 210 for **2** and 416 for **3**. Max. shift/esd=0.00. Mean shift/esd=0.00. Refinement of F^2 was done against all reflections. The weighted R-factor wR and goodness-of-fit S are based on F^2, conventional R-factors R are based on F, with F set to zero for negative F^2. The threshold expression of $F^2>2\sigma(F^2)$ is used only for calculating R-factors(gt), etc. and is not relevant to the choice of reflections for refinement. R-factors based on F^2 are statistically about twice as large as those based on F, and R-factors based on all data will be even larger. All esds (except the esd in the dihedral angle between two l.s. planes) are estimated using the full covariance matrix. The cell esds are taken into account individually in the estimation of esds in distances, angles, and torsion angles; correlations between esds in cell parameters are only used when they are defined by crystal symmetry. An approximate (isotropic) treatment of cell esds is used for estimating esds involving l.s. planes.

The main X-ray data are quoted in Table 4. For additional information regarding bond lengths and bond angles for compounds **2** and **3**, as well as the hydrogen coordinates and the anisotropic thermal parameters see the CIF files deposited as supplementary material with the Cambridge Crystallographic Data Centre. Crystallographic data (excluding structure factors) for the structures in this paper have been deposited with the Cambridge Crystallographic Data Centre as supplementary publication nos. CCDC-873346 and CCDC-873347 for compounds **2** and **3**, respectively. Copies of these data can be obtained, free of charge, on application to CCDC, 12 Union Road, Cambridge CB2 1EZ, UK, (fax: +44 (0)1223 336033 or e-mail: deposit@ccdc.cam.ac.uk).

4.3. Synthesis of (1*S*,2*R*,4*S*,5*R*,1′*S*)-2-(1-benzyloxy-2-oxoprop-1-yl)-2,4-dimethyl-8-oxabicyclo[3.2.1]octan-3-one, (1d)

Compound **1d** was synthesized according to a procedure previously developed in our research group.[8]

Table 3
Possible transition states (TS) leading to final product **3** or to its epimer **3″**

Transition State C (TS-i)		T_E, ΔH_f, E (kcal/mol)	Delta;Delta;$E^{\neq}$ (TS-i)–(TS-2) (kcal/mol)	Product
	TS-1	T_E=160.13 (MM2) ΔH_f=−67.53 (PM6) E=−651,895.9764 (DFT)	10.71 20.17 −0.05	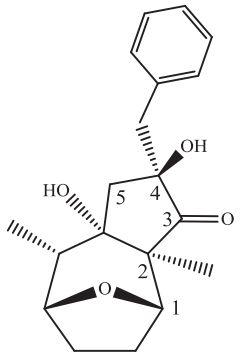 **3**
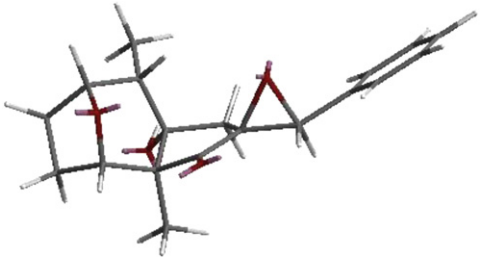	TS-2	T_E=149.42 (MM2) ΔH_f=−87.71 (PM6) E=−651,895.9277 (DFT)	0 0 0	
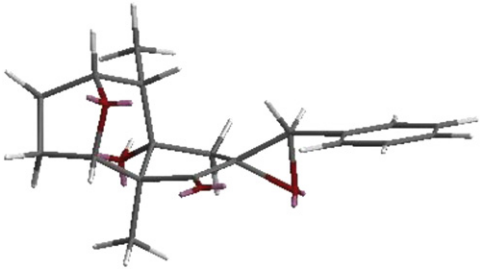	TS-3	T_E=148.60 (MM2) ΔH_f=−85.88 (PM6) E=−651,894.3678 (DFT)	−0.82 1.82 1.56	
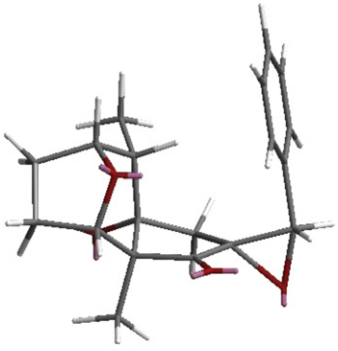	TS-4	T_E=158.53 (MM2) ΔH_f=−67.80 (PM6) E=−651,876.7375	9.11 19.91 19.19	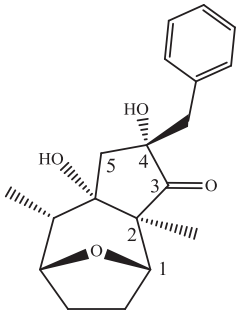 **3”**

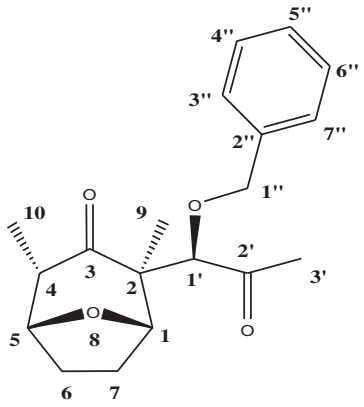

IR (film ν, cm^{-1}): 2975 (Csp^3–H, st), 1703 (C=O, st), 1476 (C–C deform), 1379, 1352, 1225, 1194, 1095, 1030 (C–O, st). ^{1}H NMR (400 MHz, $CDCl_3$, δ, ppm): 0.93 (3H, s, H9), 0.96 (3H, d, J=6.8 Hz, H10), 1.62–1.84 (4H, m, H6 and H7), 2.14 (3H, s, H3′), 3.22 (1H, dq, J_1=6.4 Hz, J_2=6.4 Hz, H4), 4.52 (1H, dd, J_1=J_2=5.6 Hz, H5), 4.56 (1H, d, J=7.6 Hz, H1), 4.71 (1H, d, J=11.2 Hz, H1″), 4.75 (1H, s, H1′), 4.77 (1H, d, J=11.2 Hz, H1″), 7.30–7.43 (5H, m, H3″ and H4″ and H5″ and H6″ and H7″). ^{13}C NMR (400 MHz, $CDCl_3$, δ, ppm): 10.10 (C10), 11.93 (C9), 24.75, 25.11 (C6 and C7), 28.08 (C3′), 48.34 (C4), 60.44 (C2), 74.95 (C1″), 80.87 (C1), 82.65 (C5), 86.78 (C1′), 128.05 (C3″ and C7″), 128.33 (C4″ and C6″), 128.79 (C5″), 137.55 (C2″), 208.37 (C3), 212.72 (C2′). MS (DIP-CI-NH_3, 70 eV, 150C, m/z (%)): 334.5 (100, M+NH_4^+), 317.5 (86.5, M+1), 209 (4, M−C_7H_7O). EA calcd for $C_{19}H_{24}O_4$: C, 72.13; H, 7.65; O, 20.23%. Found: C, 72.19; H, 7.64; O, 20.17%. TLC (SiO_2; hexane/ether, 3:7): R_f=0.49. GC (t_i=1 min; T_i=150 °C; T_f=250 °C; rate=5 °C/min; t_f=20 min): t_R=13.3 min.

Table 4
Crystal data refinement for **2** and **3**

Parameters	Compound **2**	Compound **3**
Temperature	293(2) K	293(2) K
Wavelength	0.71073 Å	0.71073 Å
Crystal system	Monoclinic	Monoclinic
Space group	*Cc*	$P2_1/c$
Unit cell dimensions	a=20.125(9)Å; α=90° b=6.419(2) Å; β=121.76(4)° c=15.359(9) Å; γ=90°	a=12.465(7) Å; α=90° b=10.761(4) Å; β=109.29(3)° c=26.134(12) Å; γ=90°
Volume	1687.0(14) Å^3	3309(3)Å^3
Z	4	8
Calculated density	1.246 Mg/m^3	1.270 Mg/m^3
Absorption coefficient	0.086 mm^{-1}	0.088 mm^{-1}
F(000)	680	1360
Crystal size	0.2×0.1×0.1 mm	0.2×0.1×0.1 mm
Theta range for data collection	2.38–30.01°	2.57–32.38°
Limiting indices	$-27\leq h\leq 28$; $-9\leq k\leq 8$; $-14\leq l\leq 21$	$-18\leq h\leq 17$; $-15\leq k\leq 13$; $-39\leq l\leq 39$
Reflections collected	4689	27,098
Independent reflections	2450 [R(int)=0.0658]	9527 [R(int)=0.0421]
Completeness to theta	(30.01°) 99.8%	(25.0°) 91.6%
Refinement method	Full-matrix least-squares on F^2	Full-matrix least-squares on F^2
Data/restraints/parameters	2450/2/210	9527/8/416
Goodness-of-fit on F^2	1.005	1.130
Final R indices [$I>2\sigma(I)$]	$R1$=0.0508; $wR2$=0.1043	$R1$=0.0678, $wR2$=0.1396
R indices (all data)	$R1$=0.1440; $wR2$=0.1304	$R1$=0.1299, $wR2$=0.1608
Largest diff. peak and hole	0.131 and −0.178 e Å^{-3}	0.223 and −0.259 e Å^{-3}

4.4. Synthesis of (1*S*,2*R*,3*R*,6*S*,7*S*,8*R*)-6-hydroxy-3-benzyloxy-2,7-dimethyl-11-oxatricyclo[6.2.1.0^{2,6}]undecan-4-one, (2)

In a 25 mL round-bottomed flask previously heated under vacuum, compound **1** (1 g, 3.16 mmol) was placed. The system was purged under argon and the product was dissolved in absolute ethanol (6 mL). In a second rounded bottom flask also previously heated under vacuum, NaOH (1.27 g, 31.8 mmol) was placed, which was subsequently dissolved in absolute ethanol (5 mL). The solution was heated at 30–40 °C in order to favor the solubility of the base. This solution was then transferred via cannula under an argon flow to the reaction flask containing the methyl ketone **1** and the operation was repeated with absolute ethanol (2 mL) in order to wash the cannula and the flask to recover the NaOH solution. The reaction mixture was stirred at room temperature for 15 h and then neutralized by adding dropwise a solution of HCl (2 M) to reach a slightly acidic pH (6–7). The crude was concentrated to dryness to remove ethanol and then redissolved in water. The resulting solution was then extracted three times with CH_2Cl_2 and the organic extract was dried over anhydrous $MgSO_4$. The organic phase was filtered and concentrated to dryness affording 0.98 g of crude mixture. The product was purified by flash column chromatography on silica gel, eluting with mixtures of hexane and diethyl ether of increasing polarity, obtaining (with H/E 30:70) 0.94 g of **2** (95%).

Mp: 122–124 °C (ether). IR (film ν, cm^{-1}): 3448 (O–H, st), 2959 (Csp^3–H, st), 1748 (C=O, st), 1466 (C–C deform), 1256, 1146, 1101 (C–O, st). ^{1}H NMR (400 MHz, $CDCl_3$, δ, ppm): 0.92 (3H, d, J=7.2 Hz, H13), 0.97 (3H, s, H12), 1.7–1.95 (3H, m, H7, H9 and H10), 2.08 (1H, d, J=19.2 Hz, H5b), 2.11–2.22 (2H, m, H9 and H10), 2.51 (1H, dd, J_1=19.2 Hz, J_2=1.6 Hz, H5b), 4.05 (1H, d, J=7.6 Hz, H1), 4.11 (1H, dd, J_1=7.6 Hz, J_2=4.0 Hz, H8), 4.62 (1H, d, J=1.2 Hz, H3), 4.69 (1H, d, J=11.6 Hz, H1′), 5.06 (1H, d, J=11.6 Hz, H1′), 7.26–7.40 (5H, m, H3′ and H4′ and H5′ and H6′ and H7′). 13C NMR (100 MHz, $CDCl_3$, δ, ppm): 10.23 (C13), 11.83 (C12), 24.00 and 24.97 (C9 and C10), 41.46 (C7), 49.18 (C5), 49.94 (C2), 73.06 (C6), 74.20 (C1′), 77.43 (C1) 79.19 (C8), 85.32 (C3), 127.87 (C3″ and C7″), 127.90 (C4″ and C6″), 128.53 (C5″), 138.42 (C2″), 213.78 (C4). MS (DIP-CI-NH_3, 70 eV, 150°C, m/z (%)): 334.5 (100, M+NH_4^+), 317.5 (13.8, M+1), 209 (2, M−C_7H_7O). EA calcd for $C_{19}H_{24}O_4$: C, 72.13; H, 7.65; O, 20.23%. Found: C, 72.11; H, 7.68; O, 20.21%. TLC (SiO_2; hexane/ether, 2:8, two elutions): R_f=0.47. GC (t_i=1 min; T_i=150 °C; T_f=250 °C; rate=5 °C/min; t_f=20 min): t_R=16.56 min.

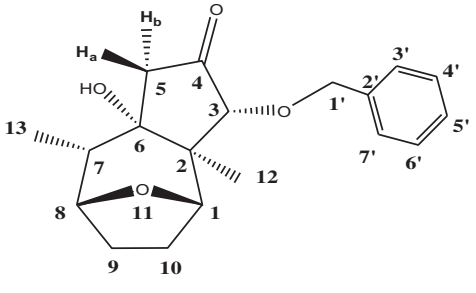

4.5. Synthesis of (1*S*,2*S*,4*S*,6*S*,7*S*,8*R*)-4-benzyloxy-4,6-dihydroxy-2,7-dimethyl-11-oxatricyclo[6.2.1.0^{2,6}] undecan-3-one, (3)

In a 100 mL round-bottomed flask previously heated under vacuum, compound **2** (0.300 g, 0.954 mmol) was placed. The

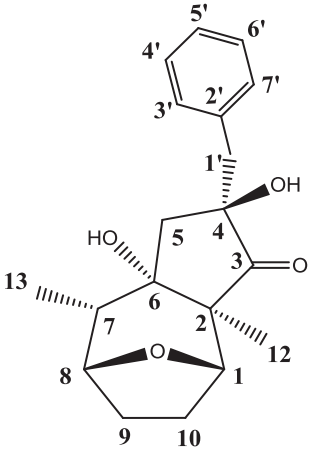

system was purged under argon and the product was dissolved in absolute ethanol (10 mL). In a second round-bottomed flask also previously heated under vacuum, NaOH (0.381 g, 9.54 mmol) was placed and subsequently dissolved in absolute ethanol (15 mL). The solution was heated at 30–40 °C in order to facilitate the solubility of the base. This dissolution was then transferred via cannula under an argon flow to the reaction flask containing the ketone **2**. The reaction mixture was stirred at room temperature for 2.5 h and then concentrated to dryness using a rotary evaporator. The obtained crude solid was dissolved in water and then neutralized by adding dropwise a solution of HCl (1 M). The resulting solution was then extracted three times with $CHCl_2$ and the organic extracts were dried over anhydrous $MgSO_4$. The organic phase was filtered and concentrated to dryness affording 0.287 g of crude mixture. The product was purified by flash column chromatography on silica gel, eluting with mixtures of hexane and diethyl ether of increasing polarity, obtaining (with H/E 1:9) 0.195 g of **3** (65%) and 0.105 g of unchanged starting material **2** (35%).

Mp: 171–173 °C (ether/hexane 2:8). IR (film ν, cm^{-1}): 3448 (O–H, st), 2959 (Csp^3–H, st), 1748 (C=O, st), 1466 (C–C deform), 1256, 1146, 1101 (C–O, st). ^1H NMR (400 MHz, $CDCl_3$, δ, ppm): 0.92 (3H, d, J=7.2 Hz, H13), 0.97 (3H, s, H12), 1.7–1.95 (3H, m, H7, H9 and H10), 2.08 (1H, d, J=19.2 Hz, H5b), 2.11–2.22 (2H, m, H9 and H10), 2.51 (1H, dd, J_1=19.2 Hz, J_2=1.6 Hz, H5b), 4.05 (1H, d, J=7.6 Hz, H1), 4.11 (1H, dd, J_1=7.6 Hz, J_2=4.0 Hz, H8), 4.62 (1H, d, J=1.2 Hz, H3), 4.69 (1H, d, J=11.6 Hz, H1′), 5.06 (1H, d, J=11.6 Hz, H1′), 7.26–7.40 (5H, m, H3″ and H4″ and H5″ and H6″ and H7″). ^{13}C NMR (100 MHz, $CDCl_3$, δ, ppm): 10.23 (C13), 11.83 (C12), 24.00 & 24.97 (C9 & C10), 41.46 (C7), 49.18 (C5), 49.94 (C2), 73.06 (C6), 74.20 (C1′), 77.43 (C1) 79.19 (C8), 85.32 (C3), 127.87 (C3″ and C7″), 127.90 (C4″ and C6″), 128.53 (C5″), 138.42 (C2″), 213.78 (C4). MS (DIP-CI-NH_3, 70 eV, 150 °C, m/z (%)): 334.5 (100, $M+NH_4^+$), 317.5 (13.8, M+1), 209 (2, $M-C_7H_7O$). EA calcd for $C_{19}H_{24}O_4$: C, 72.13; H, 7.65; O, 20.23%. Found: C, 72.15; H, 7.63; O, 20.22%. TLC (SiO_2; hexane/ether, 2:8, two elutions): R_f=0.47. GC (t_i=1 min; T_i=150 °C; T_f=250 °C; rate=5 °C/min; t_f=20 min): t_R=17.14 min.

4.6. Computational calculations

Calculations reported here were carried out using Gaussian 03W Revision E.01 (version 6.1) software.[20] All molecular ground state and transition state structures were energy preoptimized by molecular mechanics MM2 followed by semiempirical quantum mechanical PM6 algorithm,[12] implemented in the MOPAC software, and optimizing to TS. Density functional theory (DFT) based methods at the B3LYP/6–311^{++}G(d) level[21] were used for subsequent full refinements. All calculations were performed on the isolated molecules (gas phase), as consideration of solvation by the molecules of the solvent (ethanol, ε=24.5) by a polarizable continuum model (PCM)[22] produced a loss in computational performance (increase of CPU calculation time and change of convergence behavior), but did not result in significant changes of the calculated energies. As the transition states were clearly little affected by the solvent, its effect was not considered. Energies reported here are given relative to the most stable conformers of the reactants. Enthalpies (ΔH) including zero point correction, temperature correction, and vibrational energy were computed for standard conditions (T=298.15 K, P=1.0 atm). Analysis of all data and plotting of molecular structures were performed using Gaussian View 4.1 program.

Acknowledgements

We thank the Spanish Ministry of Education and Science (CTQ2007-64843/BQU) and the University of Barcelona (UB-VRR-2012/AR000126) for financial assistance. Also, a fellowship to S.P. from the Generalitat de Catalunya is gratefully acknowledged.

Supplementary data

Supplementary data associated with this article can be found in the online version, at http://dx.doi.org/10.1016/j.tet.2012.07.053. These data include MOL files and InChiKeys of the most important compounds described in this article.

References and notes

1. (a) Wittig, G.; Löhmann, L. *Liebigs Ann. Chem.* **1942**, *550*, 260–268; (b) Tomooka, K.; Yamamoto, H.; Nakai, T. *Liebigs Ann. Chem.* **1997**, 1275–1281; (c) Tomooka, K.; Yamamoto, H.; Nakai, T. *J. Am. Chem. Soc.* **1996**, *118*, 3317–3318; (d) Azzena, U.; Denurra, T.; Melloni, G.; Piroddi, A. M. *J. Org. Chem.* **1990**, *55*, 5532–5535; (e) Evans, D. A.; Baillargeon, D. J. *Tetrahedron Lett.* **1978**, 3315–3318; (f) Schafer, H.; Schöllkoft, U.; Walter, D. *Tetrahedron Lett.* **1968**, 2809–2814; (g) Schöllkopf, U. *Angew. Chem., Int. Ed. Engl.* **1970**, *9*, 763–773.
2. (a) Nakai, T.; Mikami, K. *Org. React.* **1994**, *46*, 105–209; (b) Nakai, T.; Mikami, K. *Chem. Rev.* **1986**, *86*, 885–895; (c) McNally, A.; Evans, B.; Gaunt, M. J. *Angew. Chem., Int. Ed.* **2006**, *45*, 2116–2119; (d) Maleczka, R. E.; Geng, F. *Org. Lett.* **1999**, *1*, 1111–1113.
3. Still, C.; Mitra, A. *J. Am. Chem. Soc.* **1978**, *100*, 1927–1928.
4. (a) Dunn, J. L.; Stevens, T. S. *J. Chem. Soc.* **1934**, 279–282; (b) Haslam, E.; Morris, D. G. *Biogr. Mems Fell. R. Soc.* **2003**, *49*, 521–535.
5. (a) Trost, B. M.; Ball, Z. T. *J. Am. Chem. Soc.* **2004**, *126*, 13942–13944; (b) Trost, B. M.; Bertogg, A. *Org. Lett.* **2009**, *11*, 511–513.
6. (a) Curtin, D.; Leskowitz, S. *J. Am. Chem. Soc.* **1951**, *73*, 2630–2633; (b) Curtin, D.; Leskowitz, S. *J. Am. Chem. Soc.* **1951**, *73*, 2633–2635.
7. (a) Paquette, L.; Zeng, Q. *Tetrahedron Lett.* **1999**, *40*, 3823–3826; (b) Paquette, L. A.; Pegg, N. A.; Toops, D.; Maynard, G. D.; Rogers, R. D. *J. Am. Chem. Soc.* **1990**, *112*, 277–283.
8. (a) Montaña, A. M.; Ponzano, S.; Kociok-Köhn, G.; Font-Bardia, M.; Solans, X. *Eur. J. Org. Chem.* **2007**, 4383–4401; (b) Montaña, A. M.; Fernandez, D. *Tetrahedron Lett.* **1999**, *40*, 6499–6502; (c) Montaña, A. M.; Fernandez, D.; Pagès, R.; Filippou, A. C.; Kociok-Köhn, G. *Tetrahedron* **2000**, *56*, 425–439.
9. Calculated by the SPARC algorithm: (a) Hilal, S. H.; Karickhoff, S. W.; Carreira, L. A. *Quant. Struct.-Act. Relat.* **1995**, *14*, 348–355; (b) http://ibmlc2.chem.uga.edu/sparc.
10. Calculated according to the algorithm of Marvin (ChemAxon) http://www.chemaxon.com/.
11. (a) Bailey, W. F.; Zarcone, L. M. *Tetrahedron Lett.* **1991**, *32*, 4425–4426; (b) Tomooka, K.; Yamamoto, H.; Nakai, T. *Angew. Chem., Int. Ed.* **2000**, *39*, 4500–4502; (c) Onyeozili, E. N.; Maleczka, R. E., Jr. *Chem. Commun.* **2006**, 2466–2468.
12. Calculated by using a semiempirical quantum mechanical PM6 algorithm, implemented in the MOPAC software, and optimizing to TS: (a) Dobes, P.; Rezac, J.; Fanfrlík, J.; Otyepka, M.; Hobza, P. *J. Phys. Chem. B.* **2011**, *115*, 8581–8589; (b) Stewart, J. J. P. *J. Comput.-Aided Mol. Des.* **1990**, *4*, 1–105; (c) Stewart, J. J. P. *J. Mol. Model.* **2007**, *13*, 1173–1213.
13. Calculations have been performed using a DFT (B3LYP) method using a 6-311^{++}G(d) base, implemented in the Gaussian-03 software.
14. King, J. F.; Tsang, G. T. Y.; Abdel-Malik, M. M.; Payne, N. C. *J. Am. Chem. Soc.* **1985**, *107*, 3224–3232.
15. Paquette, L. A.; Hofferberth, J. E. *Org. React.* **2003**, *62*, 477–567.
16. (a) Tomooka, K.; Igarashi, T.; Nakai, T. *Tetrahedron* **1994**, *50*, 5927–5932; (b) Verner, E. J.; Cohen, T. *J. Am. Chem. Soc.* **1992**, *114*, 375–377; (c) Hoffmann, R.; Brückner, R. *Chem. Ber.* **1992**, *125*, 1957–1963; (d) Schreiber, S. L.; Goulet, M. T. *Tetrahedron Lett.* **1987**, *28*, 1043–1046; (e) Maleczka, R. E.; Geng, F. *J. Am. Chem. Soc.* **1998**, *120*, 8551–8552.
17. (a) Suggested by one of the referees of this work: (b) Wilson, S. R. *Org. React.* **1993**, *43*, 93–250 and especially pp 144–145; (c) Koreeda, M.; Luengo, J. I. *J. Am. Chem. Soc.* **1985**, *107*, 5572–5573.
18. Sheldrick, G. M. SHELXS-97, A Computer Program for Determination of Crystal Structure, University Göttingen, Göttingen, Germany *Acta Crystallogr.* **2008**, *A64*, 112–122.
19. *International Tables of X-ray Crystallography*; Kynoch: Birmingham, UK, 1974; Vol. IV, pp 99–100 and 149.
20. Frisch, M. J.; Trucks, G. W.; Schlegel, H. B.; Scuseria, G. E.; Robb, M. A.; Cheeseman, J. R.; Zakrzewski, V. G.; Montgomery, J. A.; Stratmann, R. E.; Burant, J. C.; Dapprich, S.; Millam, J. M.; Daniels, A. D.; Kudin, K. N.; Strain, M. C.; Farkas, O.; Tomasi, J.; Barone, V.; Cossi, M.; Cammi, R.; Mennucci, B.; Pomelli, C.; Adamo, C.; Clifford, S.; Ochterski, J.; Petersson, G. A.; Ayala, P. Y.; Cui, Q.; Morokuma, K.; Malick, A. D.; Rabuck, K. D.; Raghavachari, K.; Foresman, J. B.; Cioslowski, J.; Ortiz, J. V.; Baboul, A. G.; Stefanov, B. B.; Liu, G.; Liashenko, A.; Piskorz, P.; Komaromi, I.; Gomperts, R.; Martin, R. L.; Fox, D. J.; Keith, T.; Al-Laham, M. A.; Peng, C. Y.; Nanayakkara, A.; Challacombe, M.; Gill, P. M. W.; Johnson, B.; Chen, W.; Wong, M. W.; Andres, J. L.; Gonzalez, C.; Head-Gordon, M.; Replogle, E. S.; Pople, J. A. *Gaussian 03, Revision E. 01-SMP*; Gaussian: Wallingford, CT, 2004.
21. (a) Becke, A. D. *Phys. Rev. A.* **1988**, *38*, 3098–3100; (b) Becke, A. D. *J. Chem. Phys.* **1993**, *98*, 5648–5652; (c) Lee, C.; Yang, W.; Parr, R. G. *Phys. Rev. B.* **1988**, *37*, 785–789; (d) Miehlich, B.; Savin, A.; Stoll, H.; Preuss, H. *Chem. Phys. Lett.* **1989**, *157*, 200–206; (e) Krishnan, R.; Binkley, J. S.; Seeger, R.; Pople, J. A. *J. Chem. Phys.* **1980**, *72*, 650–654; (f) McLean, A. D.; Chandler, G. S. *J. Chem. Phys.* **1980**, *72*, 5639–5648.
22. Tomasi, J.; Mennucci, B.; Cammi, R. *Chem. Rev.* **2005**, *105*, 2999–3093.